Analysis of an impulse response measured at the basilar membrane of the chinchilla (L)

Hero P. Wit[a)]
Department of Otorhinolaryngology/Head and Neck Surgery, University of Groningen, University Medical Center Groningen, P.O. Box 30.001, 9700RB Groningen, The Netherlands

Andrew Bell
John Curtin School of Medical Research, The Australian National University, Canberra, Australian Capital Territory 0200, Australia

(Received 12 March 2014; revised 20 April 2015; accepted 1 June 2015; published online 6 July 2015)

In a recent paper [J. Acoust. Soc. Am. **133**, 2224–2239 (2013)], Shera and Cooper report on the impulse response of the basilar membrane (BM) of a chinchilla, a waveform which shows repetitive bursts. They explain the bursts in terms of repeated coherent reflection at BM discontinuities and partial reflection at the stapes ("coherent reflection filtering"). Here the same waveform is examined in detail, highlighting features which indicate that the coherent reflection model, with calls for the same repetitive process to act on each successive burst, does not fully account for the shape of the measured impulse response. © *2015 Acoustical Society of America*.
[http://dx.doi.org/10.1121/1.4922469]

[KG] Pages: 94–96

In a recent paper by Shera and Cooper (2013), an impulse response of the basilar membrane (BM) of a chinchilla, measured with a displacement-sensitive laser interferometer, is shown (their Fig. 9). This figure, the only time-domain plot in the paper, gives the opportunity to investigate in detail how the waveform might be generated. For this purpose, the numerical data, shown here as Fig. 1, was kindly supplied by the authors. It comprises 1201 data points sampled at 200 kHz for 6 ms. Further analysis of the signal was done with MATHEMATICA 10 and with ABSCISSA 3.4.2 [http://rbruehl.macbay.de (last viewed 6/8/2015)].

According to Shera and Cooper (2013) the measured impulse response is the result of the superposition of "stimulus" and "delayed" components. The generation of the delayed components is illustrated in their Fig. 2: the burst following the initial burst is generated by "a distributed process of wave scattering that produces multiple wavelets that combine to form a net reverse wave that is then partially reflected at the stapes." As indicated in the figure (note the "and so on" text label), this process repeats itself several times, generating the bursts following the second. The original description of this "coherent reflection" process can be found in Zweig and Shera (1995). In this process waves are scattered at micromechanical irregularities in the BM admittance which, in the simplest case, represent "preexisting spatial irregularities in the mechanical properties of the organ of Corti."

To remove high frequency noise, the signal in Fig. 1 was first lowpass filtered with a 20th-order Butterworth filter with a cut-off frequency of 10 kHz. The result is shown as the thick line in Fig. 3. This lowpass filtered signal was subjected to a time-frequency analysis, with real-valued Morlet wavelets (details of the method can be found in Geven *et al.*, 2012), and the result is shown in Fig. 2. The dashed line in this figure, connecting local maxima, marks a frequency glide, a phenomenon often seen in BM and auditory nerve fiber click responses (Lin and Guinan, 2004).

It can be seen in Fig. 1—and more clearly in Fig. 2—that the first burst (between 0 and 1.5 ms) has a complex structure, whereas the following bursts are more regular. Our first step was therefore to decompose the signal into its five individual bursts. Because of the regularity of the signal beyond 1.5 ms, it was fitted, over the interval 1.9–5.5 ms (dashed lines in Fig. 3), as the sum of four bursts with equal-width Gaussian envelopes and single frequency f.

The formula for the fit is $g(t) = a\Sigma_{j=0}^{3} g_j(t)$, with

$$g_j(t) = \alpha^j e^{-b(t-t_0-j\Delta t)^2} \cos(2\pi f t + \phi + j\Delta\phi).$$

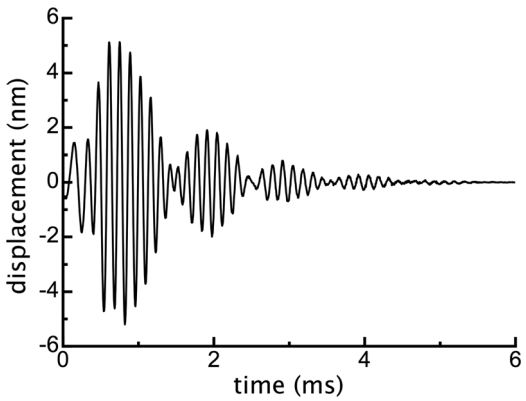

FIG. 1. Impulse response measured by Shera and Cooper (2013) at the BM of a chinchilla.

[a)]Electronic mail: hero.wit@ziggo.nl

 0001-4966/2015/138(1)/94/3/$30.00

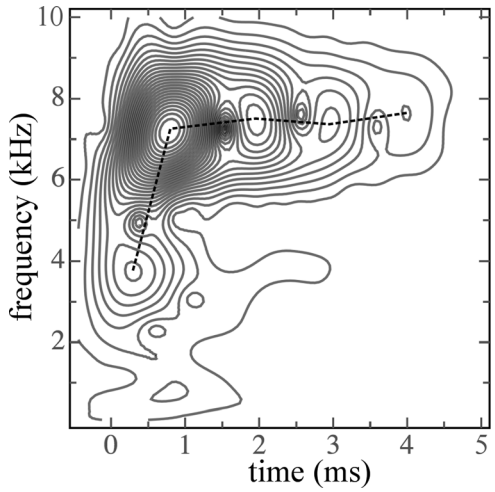

FIG. 2. Contour time-frequency plot of the waveform shown with the thick line in Fig. 3. The dashed line, connecting local maxima at 0.3, 0.8, 1.9, 2.9, and 3.9 ms, represents a characteristic "frequency glide."

This formula describes a situation in which the attenuation α, delay Δt, and phase shift $\Delta\phi$ are the same for each of the last three bursts. That is, the three bursts following the second have identical parameters with respect to the preceding burst. Parameters that gave the best least squares fit were displacement $a = 2.029$ nm, $\alpha = 0.3632$, envelope width parameter $b = 4.128\ \text{ms}^{-1}$, position of first envelope $t_0 = 1.891$ ms, $\Delta t = 1.011$ ms, $f = 7.425$ kHz, phase of first burst $\phi = -1.109$ rad, and $\Delta\phi = 3.403$ rad.

The sum of the four fitted bursts (thin line in Fig. 3) was then subtracted from the lowpass filtered original waveform (thick line in Fig. 3) to leave the first burst. The result is shown as "burst 1" in Fig. 4, which also shows the fits to the four following bursts. Thus, in this way the signal was decomposed into five separate bursts, plus a small residue.

The next step was to find a mathematical description or transfer function for the process that transforms each burst into the following one. Such a description, illustrated schematically in Fig. 5, accounts for all steps in the process (reflection at irregularities, summation of wavelets, backward travel, partial reflection, and repeated forward travel).

The (complex) transfer function $H(i\omega)$ for a linear and time-invariant system can be calculated by dividing the Fourier transform of the output signal of the system by

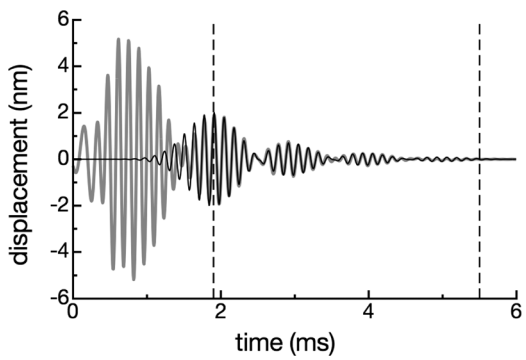

FIG. 3. Thick gray line: lowpass filtered original waveform. Thin black line: fit to the waveform interval, indicated with the dashed lines, with the sum of four cosine waves having Gaussian envelopes.

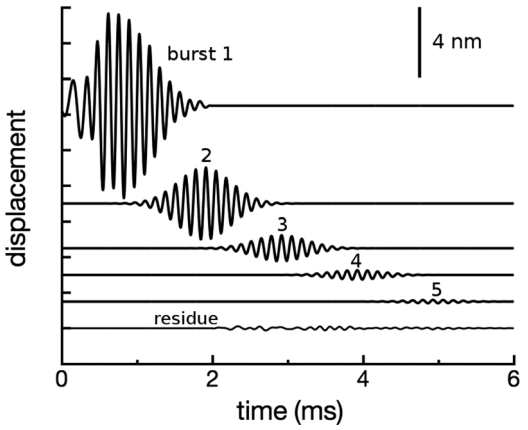

FIG. 4. Lowpass filtered original waveform decomposed into five bursts.

the Fourier transform of the input signal, so that $H(i\omega) = F[f_{out}(t)]/F[f_{in}(t)]$.

First, $H_1(i\omega)$ is calculated using burst 1 in Fig. 4 as the input signal and burst 2 as the output signal. A frequency domain illustration of the process, describing step 1 in Fig. 5, is given in Fig. 6(a): the multi-frequency burst 1 is transformed into the single-frequency burst 2. This means, as expected from Fig. 2, that step 1 involves band-pass filtering. Note also that because the amplitude spectrum of burst 2 does not completely fall within the pass-band of burst 1, it also involves amplification over a small frequency range.

Now $H_1(i\omega)$ is applied to burst 2 and the real part of the inverse Fourier transform of the outcome is calculated. The major result is that the calculated burst 3 differs substantially from the actual burst 3.

In contrast with this anomaly, if $H_2(i\omega)$ is calculated using burst 2 as the input signal and burst 3 as the output signal [Fig. 6(b)], then the fitted bursts 4 and 5 can be perfectly reconstructed by applying $H_2(i\omega)$ to burst 3 and burst 4 in turn, and calculating the real part of the inverse Fourier transform of the result. So, apart from a small residual, the waveforms of bursts 3, 4, and 5 can be explained as the result of a linear transfer process that is the same for all three bursts.

In summary, it has been shown that the transfer function $H_1(i\omega)$ for the first burst differs substantially (see Fig. 6) from transfer function $H_2(i\omega)$; however, $H_2(i\omega)$ is the same for all the following bursts and is in accordance with the assumption that bursts 3, 4, and 5 are all the result of the same sequence of processes. Bandpass filtering is an essential part of step 1 in Fig. 5, whereas steps 2, 3, and 4 involve an all-pass process, based only on delay, attenuation, and phase shift.

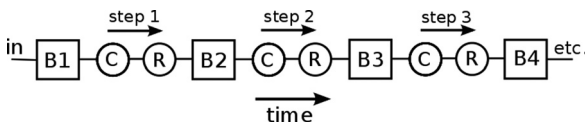

FIG. 5. Schematic representation of the process that is supposed to convert each burst into the following one. B1, B2,…: successive bursts; C: coherent reflection and summation of wavelets; R: backward travel, partial reflection at stapes, and repeated forward travel.

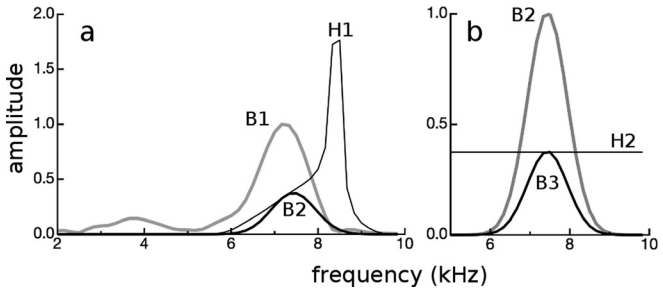

FIG. 6. (a) Thick gray line: Normalized amplitude $A_1(\omega)$ of Fourier transform $F_1(i\omega)$ of burst 1, as shown in Fig. 4. Thick black line: Amplitude $A_2(\omega)$ of Fourier transform $F_2(i\omega)$ of burst 2, scaled with respect to the maximum of A_1. Thin black line: Amplitude $A_t(\omega)$ of transfer function $H_1(i\omega)$. (A_t is the quotient of A_2 and A_1.) (b) As in panel (a), but now for burst 2 as the input signal and burst 3 as the output signal. (Resolution Δf of all spectra is 1/6 kHz.)

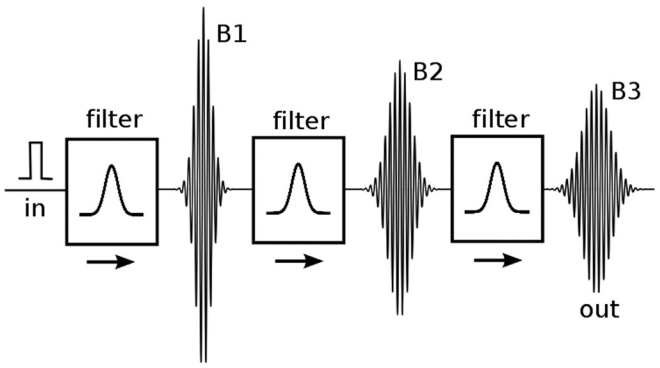

FIG. 7. B1, B2, B3: Time-domain responses of three equal Gaussian filters connected in series, if the input to the first filter is a short pulse.

It might be argued that once a signal has passed through a bandpass filter and through an identical filter again, no further signal shaping takes place. This argument is investigated in the example shown in Fig. 7, which demonstrates that each subsequent filtering step broadens the envelope of a burst. In other words, the passband of two or more identical, non-rectangular, bandpass filters connected in series is necessarily narrower than the passband of each individual filter.

We are left with the puzzling result that there is a difference between the transfer function for the first step compared to that between all the subsequent steps, and this requires explanation. The difference means that one or more components of the transfer process—reflection at fixed irregularities, summation of wavelets, backward travel along the BM, partial reflection at the stapes, and forward travel again—must depend on the parameters of the input signal. (For clarity, it is the parameters of the transfer process that are being referred to, not just the output, since it is not surprising that the output depends on the input).

This fresh analysis shows that a coherent reflection filtering model, based on a set of equal repetitive processes, cannot fully explain (at least for this particular case) why the measured burst-like impulse response has a first transfer function with a peaked and asymmetric modulus, why its peak value is larger than 1, and why there is a complete lack of filtering in the subsequent stages.

In calculating impulse responses of a one-dimensional transmission line model, Shera (2001) found an initial upward frequency glide and waxing and waning of the signal envelope (repetitive bursts), just as seen in Fig. 1 here. Repetitive bursts were only seen if random cochlear impedance perturbations were introduced (Lin and Guinan, 2004, Fig. 2). This supports the idea that irregularities are a prerequisite for generating repetitive bursts. However, this gratifying result does not imply that "coherent reflection" is the only possible description of this process.

ACKNOWLEDGMENTS

We thank Christopher Shera for supplying the data and Pim van Dijk for useful suggestions concerning the text.

Geven, L. I., Wit, H. P., De Kleine, E., and Van Dijk, P. (**2012**). "Wavelet analysis demonstrates no abnormality in contralateral suppression of otoacoustic emissions in tinnitus patients," Hear. Res. **286**, 30–40.

Lin, T., and Guinan, J. J., Jr. (**2004**). "Time-frequency analysis of auditory-nerve-fiber and basilar-membrane click responses reveal glide irregularities and non-characteristic-frequency skirts," J. Acoust. Soc. Am. **116**, 405–416.

Shera, C. A. (**2001**). "The effect of reflection emissions on impulse responses of the basilar membrane and the auditory nerve," Assoc. Res. Otolaryngol. Abs. **24**, 815.

Shera, C. A., and Cooper, N. P. (**2013**). "Basilar-membrane interference patterns from multiple internal reflection of cochlear traveling waves," J. Acoust. Soc. Am. **133**, 2224–2239.

Zweig, G., and Shera, C. A. (**1995**). "The origin of periodicity in the spectrum of evoked otoacoustic emissions," J. Acoust. Soc. Am. **98**, 2018–2047.